

Liquid Templating for Nanoparticle Organization into Complex Patterns

Camila A. Rezende,[†] Lay-Theng Lee,^{*,‡} and Fernando Galembeck[‡]

Instituto de Química, Universidade Estadual de Campinas, P.O. Box 6154, 13084-971 Campinas SP-Brazil, and Laboratoire Léon Brillouin, CEA-Saclay, 91191 Gif-sur-Yvette Cedex, France

Received August 10, 2006. In Final Form: November 23, 2006

Dewetting of thin films of charged polymer solutions produces complex patterns that can be applied to direct nanoparticle organization on solid substrates. The morphology produced by dewetting can be controlled by the solution properties, temperature, and substrate wetting. In this work, new results on this liquid-template self-assembly system are presented, with special emphasis on producing large arrays of organized nanoparticles. On a hydrophilic substrate with complete wetting, the patterns include polygonal networks and parallel-track arrays that extend over several hundreds of microns. These large structures are formed under well-controlled drying conditions and characterized by scanning electron microscopy, which is better suited for the examination of large as well as small areas than atomic force microscopy. On partial wetting substrates, new patterns are observed, including a complex set of parallel curved bands with variable particle number densities.

Introduction

Dewetting is a process that can occur in thin liquid films due to the deformability of the liquid–air interface. In this process, the free surface of an initially uniform thin film becomes unstable and is deformed, engendering the formation of a microstructure on the substrate.^{1,2} Depending on the internal interactions of the film and on the interactions with the surrounding media, the film can be stable or unstable. These interactions are assessed by considering the relevant surface and interfacial tensions. The balance of these tensions is represented by the spreading coefficient that determines the condition under which the thin liquid film dewets the substrate. While stable films are important for many surface-related technological processes like coating, adhesion, and lubrication, unstable films can be used to template micrometer and nanometer patterns in thin films.^{3,4}

Due to the technological importance of this last approach, studies on morphology evolution during the dewetting of thin liquid films over solid substrates have received widespread attention in the past years. Many theoretical^{4–6} and experimental^{3,7–11} studies have been published in the literature. For nonvolatile, apolar films deposited over homogeneous substrates, the dewetting process evolves through the following steps: the surface becomes unstable and ruptures by hole formation, the holes grow and coalesce forming a polygonal network of liquid rims, and finally the rims rupture into droplets due to Rayleigh instability.^{12,13} The rates of hole growth and coalescence as well as rim

rupture depend largely on the liquid viscosity, and droplet formation may be prevented depending on liquid viscosity. On heterogeneous substrates, with chemical and/or physical variations, the heterogeneities change the evolution of dewetting and the final morphology of the dewetted film.⁹

Techniques like microcontact printing,^{9,14,15} vapor deposition,¹⁶ monolayer chemical templates,¹⁷ and capillary force lithography¹⁸ have been used to promote inhomogeneities on substrates to organize particles. Other methods emphasize capillary forces between particles during liquid evaporation in thin liquid films.¹⁹ Nagayama²⁰ and Kralchevsky²¹ applied this method to protein systems, while Sehgal and collaborators applied it to ultrathin dewetting polystyrene films using chemically patterned substrates by microprinting progressively narrower arrays of stripes.⁹ Zhang and collaborators employed substrates with regular patterns of self-assembled monolayers produced by microcontact printing with octadecyltrichlorosilane to direct the dewetting process in thin polystyrene films, forming patterns of micrometer scale.¹⁴

Self-assembly, nanomanipulation, and chemical synthesis are the three important approaches for producing nanostructures and are therefore key processes for nanotechnology development. The reported methods to control nanoparticle self-assembly, forming open complex domains, also include the use of electric force fields,^{22,23} colloidal deposition over prepatterned substrates,^{24,25} copolymer microphases,^{26–30} electrophoresis of metallic particles in solution,²³ fluid-assisted dewetting,³¹ mi-

* Corresponding author. E-mail: laythen@dsm-mail.saclay.cea.fr.

[†] Universidade Estadual de Campinas.

[‡] Laboratoire Léon Brillouin [Laboratoire commun CEA-CNRS (UMR12)].

- (1) Sharma, A.; Jameel, A. T. *J. Colloid Interface Sci.* **1993**, *161*, 190.
- (2) Sharma, A.; Khanna, R. *Phys. Rev. Lett.* **1998**, *81*, 3463.
- (3) Karapanagiotis, I.; Gerberich, W. W.; Evan, D. F. *Langmuir* **2001**, *17*, 3463.
- (4) Bauer, C.; Dietrich, S. *Phys. Rev. E* **2000**, *61*, 1664.
- (5) Sharma, A.; Konnur, R.; Kargupta, K. *Physica A* **2003**, *318*, 262.
- (6) Kargupta, K.; Konnur, R.; Sharma, A. *Langmuir* **2001**, *17*, 1294.
- (7) Reiter, G.; Khanna, R.; Sharma, A. *J. Phys.: Condens. Matter* **2003**, *15*, 331.
- (8) Karapanagiotis, I.; Gerberich, W. W. *Surf. Sci.* **2005**, *594*, 192.
- (9) Sehgal, A.; Ferreira, V.; Douglas, J. F.; Amis, E. J.; Karim, A. *Langmuir* **2002**, *18*, 7041.
- (10) Yan, L. F. *J. Appl. Polym. Sci.* **2005**, *98*, 1412.
- (11) Reiter, G. *J. Adhes.* **2005**, *81*, 381.
- (12) Sharma, A.; Reiter, G. *J. Colloid Interface Sci.* **1996**, *178*, 383.

(13) Oron, A. *Phys. Rev. Lett.* **2000**, *85*, 2108.

(14) Zhang, Z.; Wang, Z.; Xing, R.; Han, Y. *Surf. Sci.* **2003**, *539*, 129.

(15) Yoon, B. H.; Huh, J.; Kim, H. C.; Hong, J. M.; Park, C. *Macromolecules* **2006**, *39*, 901.

(16) Zhang, F. J.; Baralia, G.; Boborodea, A.; Nysten, B.; Jonas, A. M. *Langmuir* **2005**, *21*, 7427.

(17) Yi, K. C.; Hórvölgyi, Z.; Fendler, J. H. *J. Phys. Chem.* **1994**, *98*, 3872.

(18) Luo, C.; Xing, R.; Han, Y. *Surf. Sci.* **2004**, *552*, 139.

(19) Kralchevsky, P. A.; Nagayama, K. In *Particles at Fluid Interfaces and Membranes*; Elsevier: Amsterdam, 2001; p 503.

(20) Nagayama, K. *Colloids Surf., A: Physicochem. Eng. Aspects* **1996**, *109*, 363.

(21) Kralchevsky, P. A. *Adv. Biophys.* **1997**, *34*, 25.

(22) Yeh, S. R.; Seul, M.; Shraiman, B. I. *Nature* **1997**, *386*, 57.

(23) Hermanson, K. D.; Lumsdom, S. O.; Williams, J. P.; Kaler, E. W.; Velev, O. D. *Science* **2001**, *294*, 1082.

(24) Kumar, A.; Whitesides, G. M. *Appl. Phys. Lett.* **1993**, *63*, 2002.

(25) Aizenberg, J.; Braun, P. V.; Wiltzius, P. *Phys. Rev. Lett.* **2000**, *84*, 2997.

(26) Zehner, R. W.; Sita, L. R. *Langmuir* **1999**, *15*, 6139.

crocontact printing and dewetting,³² and the formation of nanoyarns at the air–water interface using the Langmuir–Blodgett technique.^{33,34} Carbon nanotubes,^{35,36} polymeric molecules,³⁷ DNA,^{38,39} and other biomolecules^{40,41} have also been used as templates. Open arrays of nanoparticles have promising applications in the production of nanoyarns for micro- and nanoelectronic devices. Recent research in this area targets two aspects: (1) the assembly of working circuits, and (2) making elements capable of promoting electric connections between circuit parts.⁴¹

In our previous work, we studied the dewetting of charged polymer solutions on a nonmodified mica substrate.⁴² The charged polymer consists of poly(*N*-isopropylacrylamide) (PNIPAM) decorated with bound sodium dodecyl sulfate (SDS) micelles, where the polymer charge density is controlled by the surfactant-to-polymer ratio.⁴³ It is shown that thin films of this aqueous polymer solution dewet the hydrophilic mica surface, forming classic patterns that include holes, polygonal networks, and bicontinuous structures. An interesting and novel feature in the dewetted pattern consists of elongated structures that resist fragmentation into droplets; these structures are formed at high polymer charge densities. For this system, while interfacial tension and free energy aspects have been considered to explain the dewetting phenomenon, viscosity effects on its kinetics have been considered qualitatively by variation of the concentration and charge density of the polymer and of the drying rate, in relation to the formation of asymmetrical liquid structures. It is further shown that these dewetting patterns can be used to template nanoparticle organization.⁴⁴ Compared to the different methods reported in the literature, this approach is relatively simple and effective for promoting nanoparticle self-assembly into open complex patterns several tens of microns in size.

In this paper, we present new results of patterned nanoparticles obtained by this liquid-template method. By employing well-controlled drying conditions (temperature and relative humidity), large patterns spanning several hundreds of microns are obtained. The method involves confining nanoparticles in the liquid dewetting morphology, allowing capillary attractions between particles in the liquid structure upon further evaporation. The prerequisites for this two-step process are interparticle repulsion and negligible particle–substrate attraction. Interparticle repulsion, enhanced in this system by the charged molecules in the

solution, prevents the formation of particle aggregates in the bulk, even up to late-stage drying. This aspect is important because aggregates that are formed at increased concentration during drying act as “nucleation seeds” that may facilitate the development of fractal features.⁴⁵ Negligible particle–substrate attraction allows the particles to be dragged by the receding liquid during the dewetting process. For this charged system, therefore, particle patterning is driven purely by morphological changes in the liquid dewetting film. In this work, different substrates (mica, silicon, graphite) are also used to illustrate the effects of particle–substrate interaction. Scanning electron microscopy (SEM) is used to characterize the dry samples, enabling observation of large fields on the sample.

Experimental

The polymer used in this study is PNIPAM ($M_w = 90$ K), a hydrosoluble thermosensitive polymer with a lower critical solution temperature (LCST) around 32 °C. It interacts with SDS both below and above the LCST to form negatively charged PNIPAM–SDS chains with enhanced solubility in water.⁴³ The charge density on the polymer can be varied by the ratio of surfactant to polymer concentration (C_s/C_p). In the experiments reported here, the polymer concentration is fixed at $C_p = 10^{-4}$ g mL⁻¹, and the surfactant concentration varied from 5×10^{-5} , 10^{-4} , and 2×10^{-4} g mL⁻¹, corresponding to $C_s/C_p = 0.5$, 1.0, and 2.0, respectively.

Silica nanoparticles are prepared by the Stöber method described elsewhere.⁴⁶ The particle size in water determined by photon correlation spectroscopy (Zeta Plus, Brookhaven Instruments) is $d_p \approx 30$ nm. The particles are dispersed by ultrasonication in a solution containing PNIPAM and SDS at an initial particle volume fraction $\phi_p \approx 2.4 \times 10^{-5}$, corresponding to $\sim 0.006\%$ by weight.

The nanoparticle–polymer films are prepared by depositing 8 μ L of the dispersions on freshly cleaved mica, silicon wafers (Plano GmbH), or highly oriented graphite. The contact angles measured for these substrates are $\sim 0^\circ$ (mica), $43 \pm 2^\circ$ (silicon), and $54 \pm 2^\circ$ (graphite). The films are dried inside an acrylic chamber under controlled relative humidity ($50 \pm 2\%$) and temperature at 20 or 40 ± 2 °C. The dry samples are coated with Au/Pd or carbon using MED 020 equipment (Bal-Tec) and examined in a JEOL LV-JSM 6360 scanning electron microscope.

Results and Discussions

SEM is very convenient for the examination of dewetted film morphologies due to its large range of magnification and large field of observation, producing easily representative pictures of the sample. The relative ease in locating any specific region enables a large sampling of the patterns formed.

Samples Deposited on Mica: $T = 20$ °C. An aqueous solution of PNIPAM–SDS spreads spontaneously on freshly cleaved mica. Upon evaporation, the thin liquid film dewets to form patterns that depend on the polymer charge density and drying conditions (see Supporting Information). At low polymer charge density ($C_s/C_p = 0.5$) and low drying rate ($T = 20$ °C), a polygonal pattern is obtained. The formation of a polygonal network of liquid rims is one of the characteristic steps of the dewetting process that involves hole nucleation, the expansion of holes that meet to form a polygonal network, and rupture of the network resulting in hole coalescence. In the presence of silica nanoparticles, the dispersion spreads and dewets in a similar manner. During the dewetting process, the silica nanoparticles, due to their null-interaction with the mica surface, are dragged by the receding liquid and confined in the rims of the network. This

(27) Zehner, R. W.; Lopes, W. A.; Morkved, T. L.; Jaeger, H.; Sita, L. R. *Langmuir* **1998**, *14*, 241.

(28) Hamley, I. W. *Nanotechnology* **2003**, *14*, 39.

(29) Park, C.; Yoon, J.; Thomas, E. L. *Polymer* **2003**, *44*, 6725.

(30) Cheng, J. Y.; Ross, C. A.; Thomas, E. L.; Smith, H. I.; Vancso, G. J. *Adv. Mater.* **2003**, *15*, 1599.

(31) Dockendorf, C. P. R.; Choi, T. Y.; Poulikakos, D.; Stemmer, A. *Appl. Phys. Lett.* **2006**, *88*, 131903.

(32) An, L.; Li, W.; Nie, Y.; Xie, B.; Li, Z.; Zhang, J.; Yang, B. *J. Colloid Interface Sci.* **2005**, *288*, 503.

(33) Reuter, T.; Vidoni, O.; Torma, V.; Schmid, G.; Nan, L.; Gleiche, M.; Chi, L.; Fuchs, H. *Nano Lett.* **2002**, *2*, 709.

(34) Chung, S.; Markovich, G.; Heath, J. R. *J. Phys. Chem. B* **1998**, *102*, 6685.

(35) Fullam, S.; Cottel, D.; Rensmo, H.; Fitzmaurice, D. *Adv. Mater.* **2000**, *12*, 1430.

(36) Jiang, K.; Eitan, A.; Schadler, L. S.; Ajayan, P. M.; Siegel, R. W.; Grobert, N.; Mayne, M.; Reyes-Reyes, M.; Terrones, H.; Terrones, M. *Nano Lett.* **2003**, *3*, 275.

(37) Burghard, M.; Philipp, G.; Roth, S.; Von Klitzing, K. *Appl. Phys. A: Mater. Sci. Process.* **1998**, *67*, 591.

(38) Dujardin, E.; Price, R.; Yager, P.; Calvert, J. M.; Georger, J.; Singh, A. *Thin Solid Films* **1987**, *152*, 181.

(39) Schnur, J. M.; Peet, C.; Stubbs, G.; Culver, J. N.; Mann, S. *Nano Lett.* **2003**, *3*, 413.

(40) Braun, E.; Eichen, Y.; Sivan, U.; Ben-Yoseph, G. *Nature* **1998**, *391*, 775.

(41) Scheibel, T.; Parthasarathy, R.; Sawicki, G.; Lin, X.; Jaeger, H.; Linquist, S. L. *Proc. Natl. Acad. Sci. U.S.A.* **2003**, *10*, 4527.

(42) Lee, L. T.; Silva, M. C. V.; Galembeck, F. *Langmuir* **2003**, *19*, 6717.

(43) Lee, L. T.; Cabane, B. *Macromolecules* **1997**, *30*, 6559.

(44) Lee, L. T.; Leite, C. A. P.; Galembeck, F. *Langmuir* **2004**, *20*, 4430.

(45) Mougín, K.; Haidara, H. *Langmuir* **2002**, *18*, 9566.

(46) Costa, C. A. R.; Leite, C. A. P.; Galembeck, F. *J. Phys. Chem. B* **2003**, *107*, 4747.

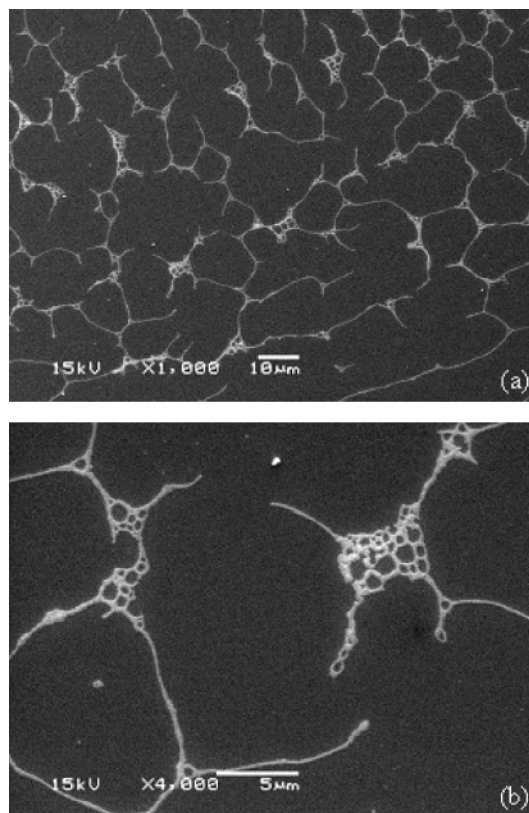


Figure 1. SEM images of silica nanoparticles deposited on mica from a PNIPAM–SDS solution at low polymer charge density ($C_s/C_p = 0.5$) and dried at $T = 20$ °C: (a) magnification $1000\times$, scale bar = $10\ \mu\text{m}$; (b) magnification $4000\times$, scale bar = $5\ \mu\text{m}$.

liquid template, upon drying, sets the nanoparticles in the polygonal network structure (Figure 1).

The remarkable feature of this sample is the large area over which the pattern is formed on the substrate, indicating a high degree of surface chemical homogeneity as well as good control of the drying conditions. Increased magnification of the image (Figure 1b) shows regions that correspond to two-dimensional “plateau borders” in liquid foams. Capillary forces at these borders are responsible for the drainage of liquid from the rims to the rim intersections where the pressure is lower, due to the Young–Laplace equation. These regions are thicker and therefore dewet later, as can be seen from its hole nucleation stage, while other regions are already in an advanced stage of dewetting.

At increased polymer charge density ($C_s/C_p = 1.0$), the nanoparticles form tracks consisting of elongated structures that vary from a few to several tens of microns in length (Figure 2a). The quasi-periodicity and bifurcation points indicate that this pattern also originates from the rupture of the rims of a polygonal network.

Upon further increase in polymer charge density ($C_s/C_p = 2.0$), while keeping the drying temperature at 20 °C, extended elongated structures predominate. These structures result from rims that resist fragmentation, probably due to viscous effects opposing the Rayleigh instability that causes the rupture of elongated structures into droplets. The increased polymer charge density probably contributes to these effects. These “silica yarns” with very high aspect ratios are aligned with long-range order at about $20\ \mu\text{m}$ periodicity (Figure 2b). Note that these “yarns” average about $80\text{--}100\ \text{nm}$ in height, as measured by atomic force microscopy.⁴⁴ Since the particle diameter is about $30\ \text{nm}$, the yarns are multiparticle chains. These parallel patterns extend over a large area on the mica surface and are very reproducible.

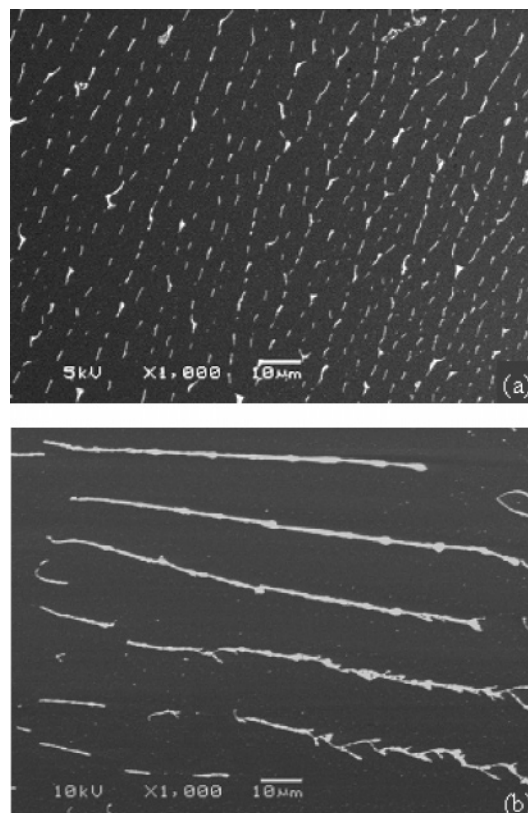


Figure 2. SEM images of silica nanoparticles deposited on mica from a PNIPAM–SDS solution at (a) $C_s/C_p = 1.0$, (b) $C_s/C_p = 2.0$, and dried at $T = 20$ °C. Magnification $1000\times$, scale bar = $10\ \mu\text{m}$.

Similar structures with defined distance between parallel tracks have also been reported by Karthaus and collaborators for polystyrene dissolved in benzene deposited over mica and kept above the glass transition temperature of the PS.⁴⁷

Samples Deposited on Mica: $T = 40$ °C. When the samples are dried at 40 °C, the increased evaporation rate accelerates dewetting and favors the formation of elongated structures. This is shown in Figure 3 for a sample at low charge density ($C_s/C_p = 0.5$). Here, the polygonal network seen in Figure 1 evolves toward a parallel-track pattern, a result of the high anisotropy of the liquid forming the polygonal rims, due to chain alignment. These track patterns extend even to the border of the film, as shown in Figure 3b. The absence of a “drying front”-type structure on this sample indicates good spreading and uniform film thickness and dewetting up to the border. At increased charge density ($C_s/C_p = 1.0$), similar parallel-track structures are obtained, although, at this charge density, this type of structure has already been observed at 20 °C. Thus, an increase in drying rate induces an effect similar to that caused by an increase in polymer charge density, with both parameters favoring the formation of elongated structures. This shows the importance of viscosity effects in structure formation, since increasing drying rate reduces the time for the liquid patterning as the film reaches very high viscosity without breaking into droplets.

The patterns that are obtained in this study extend over a very large area of the substrate. This is a highly desirable quality that is achieved in the present work by using well-controlled drying conditions. Nevertheless, although inhomogeneity and nonuniform drying effects can be minimized, they are almost impossible

(47) Karthaus, O.; Grasjö, L.; Maruyama, N.; Shimomura, M. *Chaos* **1999**, *9*, 308.

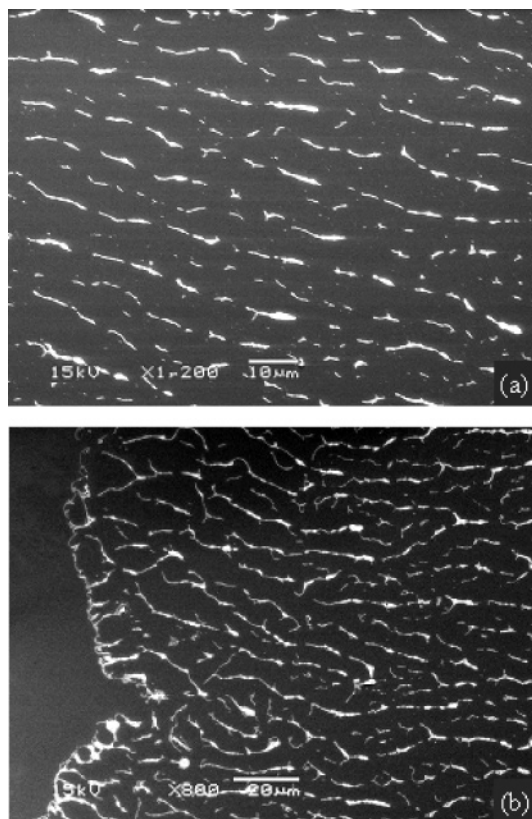


Figure 3. SEM images of silica nanoparticles deposited on mica from a PNIPAM-SDS solution at $C_s/C_p = 0.5$, $T = 40$ °C: (a) magnification 1200 \times , scale bar = 10 μm ; (b) film border, magnification 800 \times , scale bar = 20 μm .

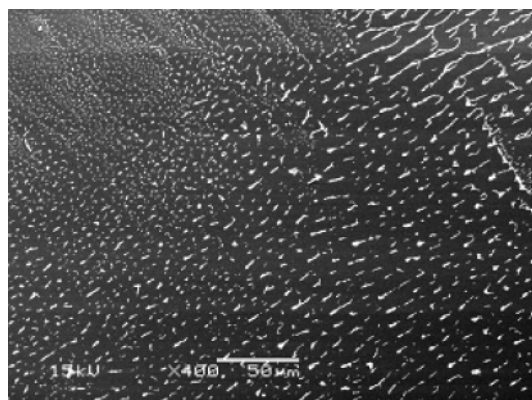


Figure 4. SEM image of silica nanoparticles deposited on mica from PNIPAM-SDS solution at $C_s/C_p = 0.5$ and $T = 40$ °C showing parallel-track and particulate patterns on the same sample. Magnification 400 \times , scale bar = 50 μm .

to eliminate completely, unless all sample preparation and handling are performed under clean room conditions with mechanical or automated handling conditions that are not justified at this stage of this project. It is common to observe different patterns on the same substrate due to uneven thickness and drying that engender different dewetting morphologies, or due to local chemical heterogeneity that modifies the wetting behavior of the liquid as well as the particle-surface interactions. This is seen in Figure 4 for a sample dried at 40 °C where parallel-track and particulate patterns coexist on the same sample.

Samples Deposited on Silicon and Graphite. To study the influence of the nature of substrate on nanoparticle organization, silicon and graphite substrates are used. When an aqueous dispersion containing polymer and nanoparticles is deposited on

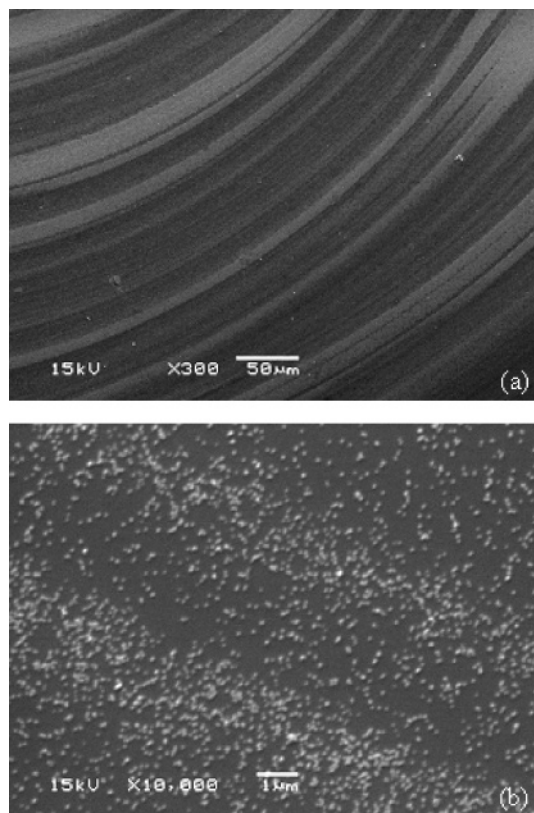


Figure 5. SEM images of silica nanoparticles deposited on silicon from a PNIPAM-SDS solution at $C_s/C_p = 2.0$, $T = 40$ °C: (a) magnification 300 \times , scale bar = 50 μm ; (b) magnification 10000 \times , scale bar = 1 μm .

silicon, poor spreading is observed, as expected, in view of its less hydrophilic nature. The dry sample border forms a macroscopic circular trace that is visible to the eye. SEM imaging shows that samples with different charge densities dried at different temperatures show little differences in characteristics. Figure 5 shows an image of a sample at high polymer charge density ($C_s/C_p = 2.0$) dried at 40 °C. While excess material is accumulated in the center of the droplet, the border shows partial wetting with a series of circular bands. A magnification of the border shows that the bands consist of disperse particles deposited on the substrate. Interestingly, successive bands with different particle densities are formed, suggesting that the effectiveness of particle dragging may vary between dewetting stages. This oscillatory behavior has not been observed previously in dewetting studies but is very attractive for application reasons. It is reminiscent of two different well-known types of spatial patterns formed under nonequilibrium conditions: Liesegang rings and structures formed under slip-stick behavior. In the present case, the fact that the particles are not dragged by the receding film to form well-defined rings at the drying front indicates particle adhesion to the substrate.

On an even less hydrophilic substrate such as graphite, the dispersion does not spread, and all regions remain relatively thick. The morphology of the dry drop shows no feature of thin film dewetting; rather, it consists of a polymer network with disperse nanoparticles deposited on the substrate (Figure 6). As in the case of silicon, this morphology does not vary between different samples and drying conditions.

The film morphologies obtained on silicon and graphite surfaces provide important information that can help explain random features that are sometimes observed along with samples that form organized structures. In some cases, different organized

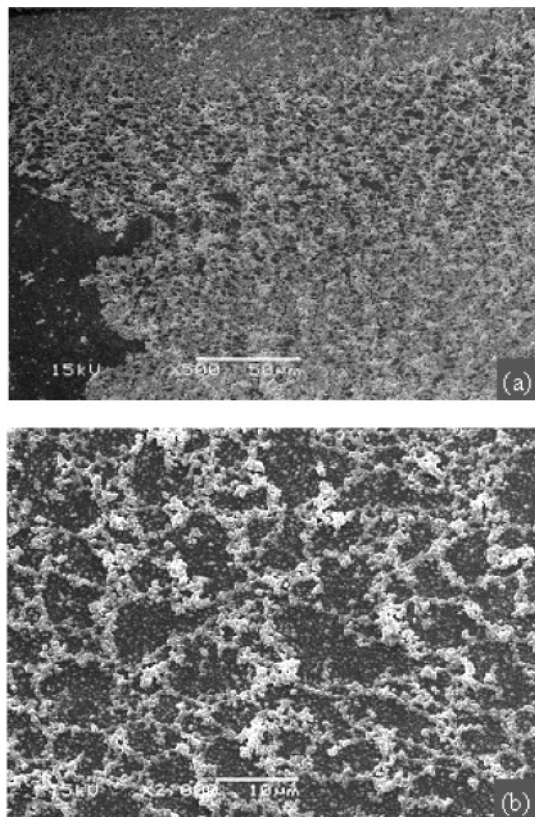


Figure 6. SEM images of silica nanoparticles deposited on graphite from a PNIPAM–SDS solution at $C_s/C_p = 0.5$, $T = 40\text{ }^\circ\text{C}$: (a) magnification $500\times$, scale bar = $50\text{ }\mu\text{m}$; (b) magnification $2000\times$, scale bar = $10\text{ }\mu\text{m}$.

patterns coexist due to uneven film thicknesses that engender different dewetting patterns (especially on ultrathin films), but other morphologies due to surface chemical inhomogeneity are almost unavoidable. Even mica freshly cleaved under laboratory

conditions is highly susceptible to contamination and substrate chemical inhomogeneity, giving rise to reduced hydrophilicity that can result in partial wetting of aqueous solutions and particle–substrate interactions. Last but not least, these findings can also be helpful for producing surfaces with well-defined nanostructures that can in turn be used to make topology-assisted superhydrophobic surfaces.⁴⁸

Conclusions

The dewetting of charged polymer solutions from a hydrophilic substrate offers a potential method for organizing nanoparticles into two-dimensional complex patterns. Depending on the polymer charge density and drying rate, polygonal patterns and parallel-chain arrays can be obtained. Under well-controlled drying conditions, these reproducible patterns extend over several hundred microns in size. Since the process works by confinement of the nanoparticles within the liquid dewetting structures, particle–substrate repulsion facilitates the process, while particle–substrate adhesion prevents the receding front of the dewetting liquid from dragging the particles with it. A good spreading coefficient of the liquid on the substrate is also necessary for producing large patterns, as it ensures uniform film thickness, an important parameter that controls the dewetting pattern. Less hydrophilic substrates with poor spreading coefficients do not engender complex dewetting patterns of an aqueous solution, and particle adhesion can also occur during the drying process.

Acknowledgment. The authors thank FAPESP, CAPES, and the Millennium Institute of Complex Materials for financial support.

Supporting Information Available: AFM images of the dewetting of PNIPAM–SDS solutions on mica. This material is available free of charge via the Internet at <http://pubs.acs.org>.

LA062370S

(48) Teare, D. O.H.; Spanos, C. G.; Ridley, P.; Kinmond, E. J.; Roucoules, V.; Badyal, J. P. S.; Brewer, S. A.; Coulson, S.; Willis, C. *Chem. Mater.* **2002**, *14*, 4566.